J Mater Sci (2010) 45:2285–2295
DOI 10.1007/s10853-009-4190-4

Effect of magnesium content on thermal and structural parameters of Al–Mg alloys directionally solidified

Jean Robert Pereira Rodrigues · Mirian de Lourdes Noronha Motta Melo · Rezende Gomes dos Santos

Received: 18 June 2009 / Accepted: 30 December 2009 / Published online: 14 January 2010

Abstract In this study, the influence of magnesium content on thermal and structural parameters during the unsteady-state unidirectional solidification of Al–Mg alloys is analyzed. Using a special device, Al–Mg alloys containing 5, 10, and 15 wt% Mg were submitted to unidirectional solidification. Using a data acquisition system, the temperature variations along the casting during solidification were measured. From these results, the variations of solidification parameters as growth rate of dendrite tips, thermal gradient, cooling rate, and local solidification time were determined. The variation of global heat transfer coefficient at metal/mould interface was estimated through the adjustment of experimental temperature variation close to the interface and numerical predictions. Primary and secondary dendrite arms spacing variations during solidification were measured by optical microscopy. From these results, comparative analysis were developed to determine the influence of magnesium content.

J. R. P. Rodrigues
Department of Mechanical Engineering (DEMECP), CCT, State University of Maranhão (UEMA), Av. Lourenço Vieira da Silva, S/N, 65055-310 Sao Luiz, MA, Brazil

M. de Lourdes Noronha Motta Melo
IEM, Federal University of Itajuba (UNIFEI), Av. BPS, 1303, 37500-903 Itajuba, MG, Brazil

R. G. dos Santos (✉)
Department of Materials Engineering (DEMA), School of Mechanical Engineering (FEM), University of Campinas (UNICAMP), P.O. Box 6122, 13083-970 Campinas, SP, Brazil
e-mail: rezende@fem.unicamp.br

Introduction

The understanding of variation of thermal parameters and their influence on mechanisms of microstructure evolution during solidification of metallic alloys is important in modern casting technology to improve the quality of metal castings, since the resultant properties depend markedly on the final structure [1, 2]. The parameters that affect microstructure formation are the dendrite tips growth rate, thermal gradient ahead of solid/liquid interface, cooling rate, and local solidification time. Monitored unidirectional solidification is a powerful experimental technique and has been widely applied to analyze the correlation between these parameters and the microstructure formation [3]. During solidification of metallic alloys, a substantial change in solute concentration is observed ahead of the solid/liquid interface, affecting the local equilibrium liquidus temperature [1, 2]. The liquidus temperature increases with the distance from the interface. Depending on the alloy this change in concentration can reach a long extension. Ahead of the interface may exist a zone affected by constitutional supercooling. This zone represents a volume of melt ahead of interface in which the real temperature of the liquid is lower than the local equilibrium liquidus temperature. The liquid in this zone is undercooled, thus in a metastable state, given rise to a mushy zone and leading to a dendritic structure and to microsegregation between dendritic arms [2]. During the last decades several studies have been developed to analyze solid/liquid interface morphology, growth conditions, instabilities at solid/liquid interface, and to correlate primary and secondary dendrite arms evolutions with solidification conditions. Melo et al. applied unsteady-state unidirectional solidification to analyze dendrite arm spacing variation and microporosity formation in Al 4.5 wt% Cu

alloys, proposing a numerical method to predict dendrite arm spacing and position, amount and size of microporosity formed both by dissolved gases and solidification shrinkage [4, 5]. The authors concluded that for a given initial hydrogen content, the volumetric fraction of pores and the size of pores decreases as cooling rate increases and that for cooling rates below 11 °C/s, the volume of porosity formed by dissolved gases increases abruptly. Rocha et al. studied cellular/dendritic transition in Sn–Pb alloys and the influence of heat flow parameters on dendrite spacing in Sn–Pb and Al–Cu alloys during unsteady-state solidification [6, 7]. The authors concluded that cellular/dendritic transition occur for the Sn 2.5 wt% Pb alloy over a range of cooling rate from 0.5 to 5.2 K/s. They also established theoretical conditions for cellular/dendritic transition in Sn–Pb alloys. Gündüz and Çadirli solidified unidirectionally different Al–Cu alloys under steady-state conditions and correlate experimental results for dendrite arm spacing, dendrite tip radius, and mushy zone depth with solidification parameters, using linear regression [8]. Whitesell and Overfelt analyzed the influence of solidification variables on microstructure, macrosegregation, and porosity formation in directionally solidified bars of nickel-base superalloy [9]. They imposed, in each experiment, a constant growth rate obtaining constant interdendritic spacing. From the results, they establish better conditions to minimize pore formation. Lin et al. studied the influence of solidification rate on primary cellular and dendritic spacing solidifying different aluminum alloys directionally in a vacuum Bridgman apparatus [10]. They concluded that for a given growth condition, there is a wide range of primary spacing for both cellular and dendritic growth.

Henry et al. analyzed different aluminum alloys, including Al–Cu, Al–Mg, and Al–Si, directionally solidified under controlled thermal and convection conditions, observing particular growing morphologies for relatively high solidification rates [11]. Specially for the 5182 Al–Mg type alloy, they observed not twinned columnar grains together with feathery crystals. The authors concluded that these so-called exotic morphologies in aluminum alloys are probably due to small anisotropy of the surface tension of the solid–liquid interface.

Most of the articles cited previously, apply the unidirectional solidification technique to study different aspects of solidification parameters' variations during the solidification of metallic alloys and their influences in the macro and microstructure formation. In spite of the technological importance of Al–Mg alloys, not many publications concerned to the analysis of the solidifications process of these alloys are found in literature. The knowledge of the influence of alloy content on solidification parameters and on microstructure formation is particularly important due to the influence on final mechanical properties. In the present study, unsteady-state unidirectional solidification of Al–Mg alloys is used to analyze the influence of magnesium content on thermal and structural parameters during solidification process. Temperature variations along the casting were measured during solidification. From the casting temperature data, the variations of solidification parameters as growth rate of dendrite tips, thermal gradient ahead of dendrite tips, cooling rate, and local solidification time were determined. The variation of global heat transfer coefficient between the solidifying alloy and the coolant at metal/mould interface was estimated through the adjustment of experimental temperature variation close to the interface and numerical predictions, by using the inverse method. Primary and secondary dendrite arms spacing variations during solidification were measured by optical microscopy. The results obtained permitted to establish the influence of magnesium content on the thermal parameters, on the columnar/equiaxial transition and on dendrite arm spacing.

Experimental procedure

Three Al–Mg alloys were prepared containing 5, 10, and 15 wt% Mg. Some experiments were conducted also with pure aluminum for comparisons concerning to columnar/equiaxial transition. The samples were directionally solidified using a experimental device, showed schematically in Fig. 1. This device was successfully used in previous

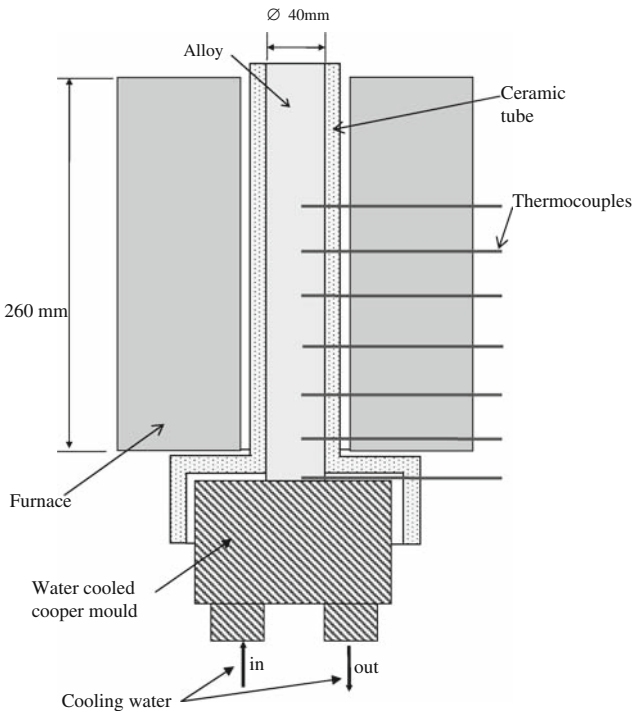

Fig. 1 Schematic representation of the experimental device used to promote upward unidirectional solidification

studies [4, 5]. The alloys were melted and poured in a cylindrical ceramic tube with an internal diameter of 40 and 260 mm in length, positioned over a water-cooled cooper mould which promotes upward unsteady-state directional solidification. The cylindrical ceramic tube is placed in a furnace and kept at 600 °C for pure aluminum and 550 °C for the Al–Mg alloys, before the beginning of the solidification to minimize radial heat losses. In order to initiate solidification process, the electric heaters of the furnace are disconnected when the water flow is initiated. A superheat of about 10% was adopted in all experiments, which mean initial temperatures equal to 720 °C for pure aluminum and 650, 670, and 700 °C for the alloys with 15, 10, and 5% Mg, respectively. Argon was injected in the melt before pouring to eliminate dissolved gases. Temperature variations during solidification were measured using chromel–alumel thermocouples coupled to a data acquisition system, positioned along the centerline of the cylindrical ceramic tube containing the sample, at metal/mould interface and at distances of 2, 20, 40, 60, 80, 100, and 120 mm from this interface.

The macro and microstructures were analyzed through optical microscopy. The longitudinal sections of the solidified specimens were polished and etched for macroscopic examination. Pure aluminum was etched with a reagent containing 45% HCl, 15% HNO_3, 15% HF and 25% water, and Al–Mg alloys with a reagent containing 20 mL glycerin, 30 mL HCl, 2 mL saturated water solution $FeCl_3$, 1 mL HNO_3 and HF (7 drops). Selected samples of the longitudinal sections were polished and etched for microscopic examinations of Al–Mg alloys. The alloy containing 5 wt% Mg was etched with a reagent containing 20 mL H_2O, 1 mL HF, 6 mL HNO, and 12 mL HCl and the alloys containing 10 and 15 wt% Mg with a 10% HF water solution.

Dendrite arm spacing were measured using image processing system Neophot 32 (Carl Zeiss, Esslingen, Germany) and Leica Quantimet 500 MC (Leica Imaging systems Ltd., Cambridge, England) adopting the method proposed by Gündüz and Çardili [8].

Results and discussions

Figure 2 shows experimental set of cooling curves, obtained using thermocouples and the data acquisition system, for Al 5 wt% Mg (a), Al 10 wt% Mg (b), and Al 15 wt% Mg (c). From these curves, it is possible to determine the positions of the liquidus isotherm, that means the position of dendrite tip, as function of time. The liquidus temperature for each alloy is indicated on the corresponding figures.

From the experimental results for temperature variations in the casting during solidification, the variation of global

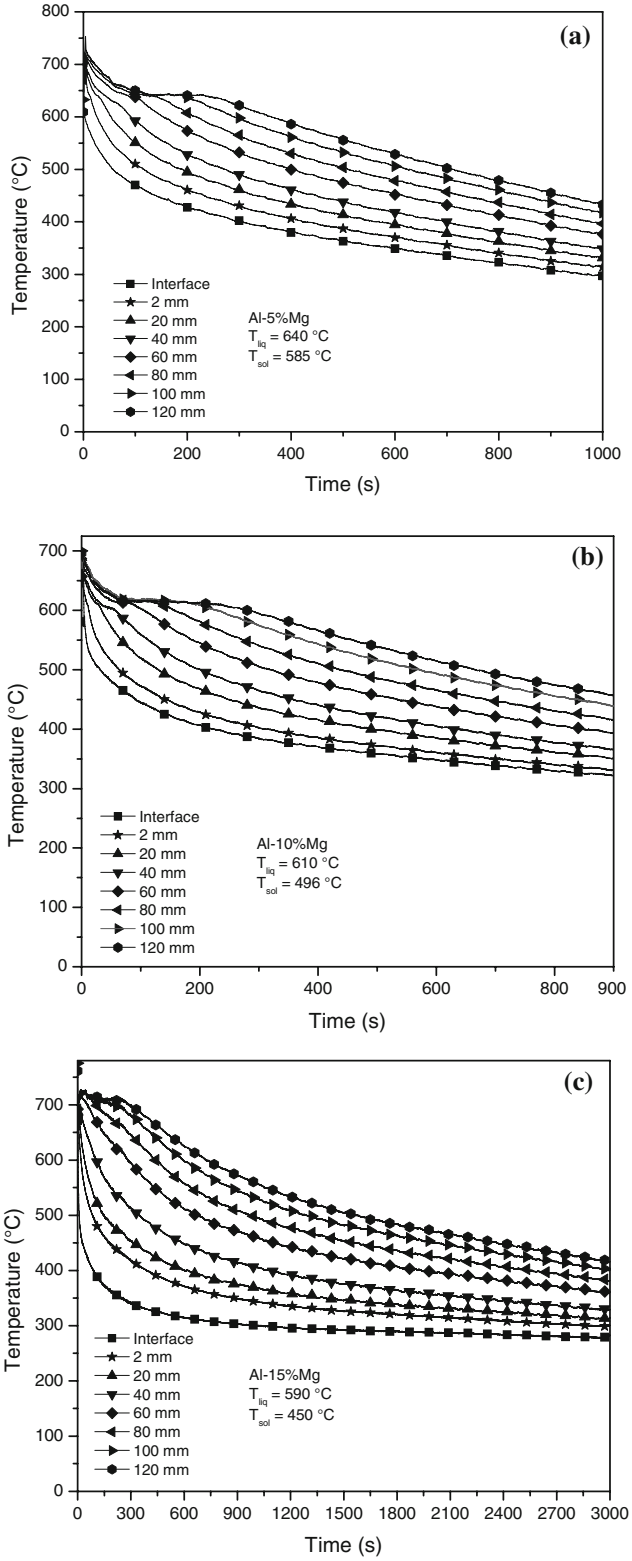

Fig. 2 Experimental set of cooling curves obtained for Al with 5, 10 and 15 wt% Mg

heat transfer coefficient between the solidifying alloy and the coolant at metal/mould interface (h_i) was determined for the three alloys applying numerical simulation and the

inverse method [12, 13]. Accurate measurements of temperature at several points in the casting, which depend on the heat transfer coefficient, were used for determination of this coefficient. Considering the efficient flow in the water-cooled cooper mould, the temperature of the mould in contact with the water is adopted as 25 °C during the solidification process. The heat transfer coefficient is manipulated to adjust the numerical prediction of the temperatures to the experimental data. This heat transfer coefficient represents an overall value between metal and coolant, including the influences of air gap, cooper sheet, and water/mould thermal resistance.

The numerical method used is the same applied in previous articles by the authors [4, 5]. Basically, it was developed considering the energy conservation equation at macroscopic scale given by:

$$\rho \cdot c_p \cdot \frac{\partial T}{\partial t} = \nabla \cdot (k \cdot \nabla T) + Q \tag{1}$$

where ρ is the density of the alloy, c_p is the specific heat, k is the thermal conductivity, Q is the heat liberated during solidification, T is temperature, and t is time. The heat liberated during solidification is taken into account applying the enthalpy method [13]. The fraction of solid (f_s) as function of temperature is determined using the Scheil equation [14]. Using the enthalpy method, the Eq. 1 can be put in the following form:

$$\frac{\partial H}{\partial T} = \rho \cdot c_p - \rho \cdot L \cdot \frac{\partial f_s}{\partial t} \tag{2}$$

where H is enthalpy, L is latent heat of solidification, and f_s is fraction of solid. This equation permits to treat continuously solidified metal, mushy zone, and liquid metal. At metal/mould interface, the following energy balance is established:

$$-k \cdot \frac{\partial T}{\partial x} = h_i \cdot (T_m - T_0) \tag{3}$$

where h_i is the global heat transfer coefficient between the alloy and the coolant, T_m is the temperature of the alloy at metal/mould interface and T_0 is the temperature of the coolant.

Considering variable thermophysical properties in the alloy, published by Pehlke [15], and variable heat transfer coefficient between solidifying alloy and coolant at metal/mould interface and following a suitable discretization of metal/mould system, the differential equations are solved using finite difference method, and values of enthalpy variation in the sample as function of position and time are obtained. The variation of temperature in the sample is obtained from the values of enthalpy using a curve of variation of enthalpy versus temperature of the alloy, previously calculated from the variation of specific heat with temperature.

The determination of temperature variation in the sample during solidification process is also important because from these results the variations of solidification parameters as growth rate of dendrite tips, thermal gradient ahead of dendrite tips, cooling rate, and local solidification time are determined. These parameters are important to analyze the influence of metal/mould characteristics on solidification process.

Figure 3 shows the time dependence of the global heat transfer coefficient between metal and coolant for the Al–Mg alloys containing 5, 10, and 15 wt% Mg. It is observed that the coefficient increases significantly as magnesium content increases. This behavior is probably consequence of the improvement of wetting of the alloy as the magnesium content increases, optimizing the contact between metal and mould. For all the alloys, the heat transfer coefficient decreases drastically with the time due to the increasing of the air gap in the metal/mould interface as consequence of the contraction of the alloy during solidification.

The experimental results of temperature variation in the alloy have been used also to estimate the variation of other important parameters during the solidification process, as displacement of liquidus isotherm, growth rate of dendrite tip, local solidification time, cooling rate, and thermal gradient ahead of dendrite tip.

Figure 4 shows the position of the liquidus isotherm (s) as function of time (t) for the different Al–Mg alloys, obtained from the set of cooling curves. From the experimental data of temperature variation, it is determined that the time necessary for the liquidus isotherm reach each position in the sample. It is observed that increasing the magnesium content, which increases the difference

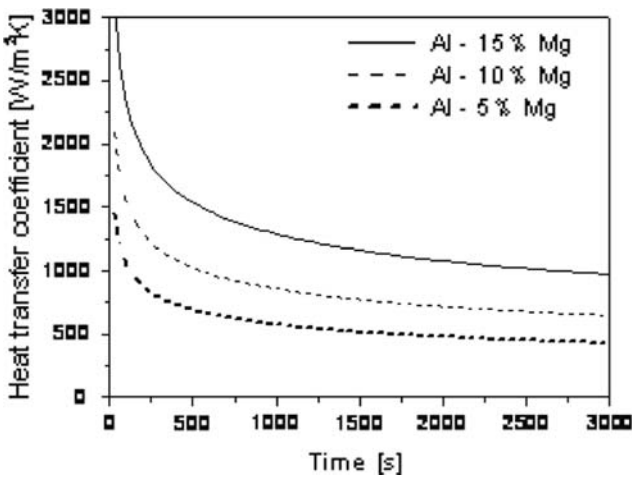

Fig. 3 Variation of heat transfer coefficient at metal/mould interface as function of time for the Al–Mg alloys containing 5, 10 and 15 wt% Mg

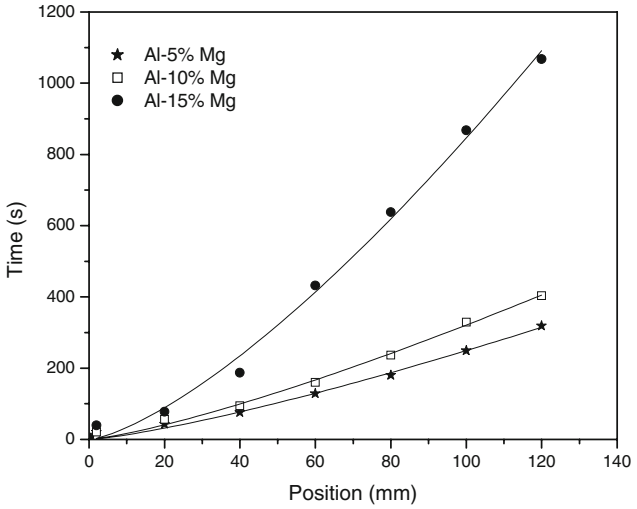

Fig. 4 Position of the liquidus isotherm (s) as function of time (t) for the different Al–Mg alloys

between liquidus and solidus temperatures, the time for the dendrite tips reach an equivalent distance also increases. Increasing the difference between solidus and liquidus temperature, the zone affected by constitutional supercooling, in which the real temperature of the liquid is lower than the local equilibrium liquidus temperature, increases giving rise to a extended mushy zone with heat conduction smaller than the solid zone, decreasing the heat flow. As a consequence, the dendrite tip growth rate (v) decreases as magnesium content increases, as it can be observed in Fig. 5, increasing the time for dendrite tips reach an equivalent distance.

Figure 5 shows the dendrite tip growth rate (v) as function of the position of liquidus isotherm. The dendrite tip growth rate is obtained from the experimental data for temperature variation in the sample during solidification process applying the relation:

$$v = \frac{x_2 - x_1}{t_2 - t_1} \tag{4}$$

where $x_2 - x_1$ is the distance between two positions, 1 and 2, of the dendrite tip in the sample and $t_2 - t_1$ is the time necessary for the displacement of the dendrite tip (liquidus isotherm) from position 1 to position 2. The results show that the cooled mould imposes a high heat extraction close to metal/mould contact, leading to a high growth rate. This growth rate decreases along the solidification process due to the increasing thermal resistance both at the interface, as consequence of air gap formation, and to the increasing solidified shell. It is also observed that increasing the magnesium content decreases the growth rate, due to the extended mushy zone as explained above. This is coherent with the results for displacement of liquidus isotherm presented in Fig. 4.

The local solidification time (t_l) represents the time interval between the passage of liquidus and solidus isotherms in a given position in the casting. The variations of local solidification time as function of position of liquidus isotherm for the three Al–Mg alloys are presented in Fig. 6. The results show that local solidification time increases with increasing magnesium content. The reason is related to the influence of increasing alloy content on the difference between solidus and liquidus temperature. The increasing in the difference between solidus and liquidus temperature and the constitutional super cooling lead to an increasing in the extension of the mushy zone, as previously explained, and consequently the time interval necessary to the dendrites tips and roots pass to a given position increases.

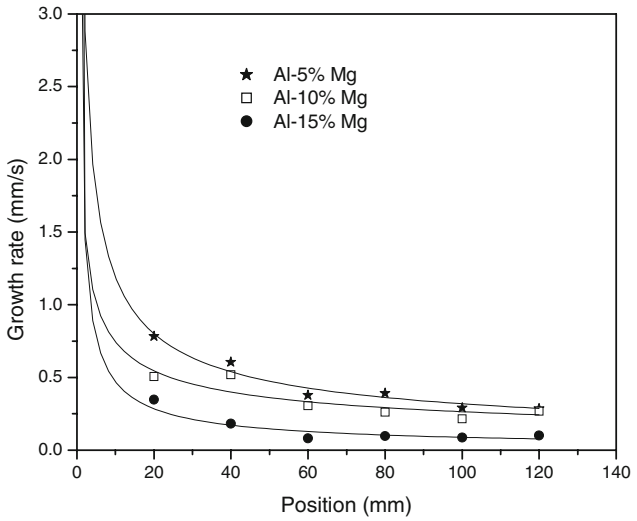

Fig. 5 Dendrite tip growth rate (v) as function of the position of liquidus isotherm (s) for the different Al–Mg alloys

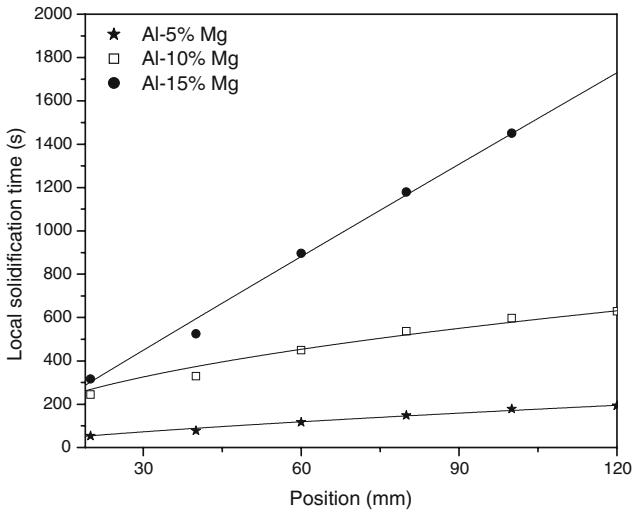

Fig. 6 Variations of local solidification time (t_l) as function of the position of liquidus isotherm (s) for the different Al–Mg alloys

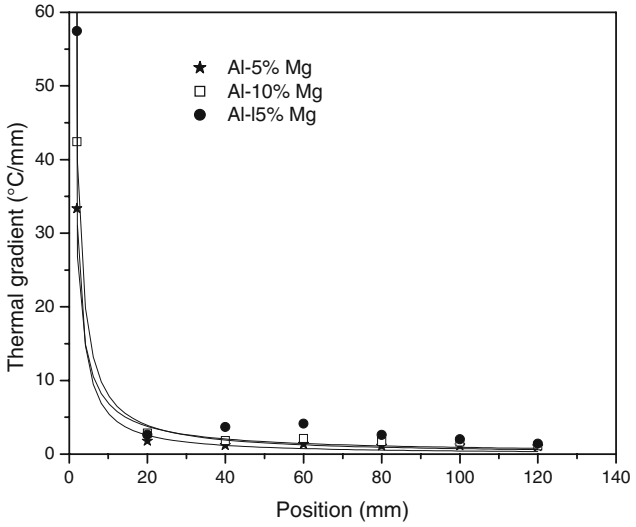

Fig. 7 Variations of thermal gradient (G_L) ahead of liquidus isotherm as function of the position of this isotherm (s) for the different Al–Mg alloys

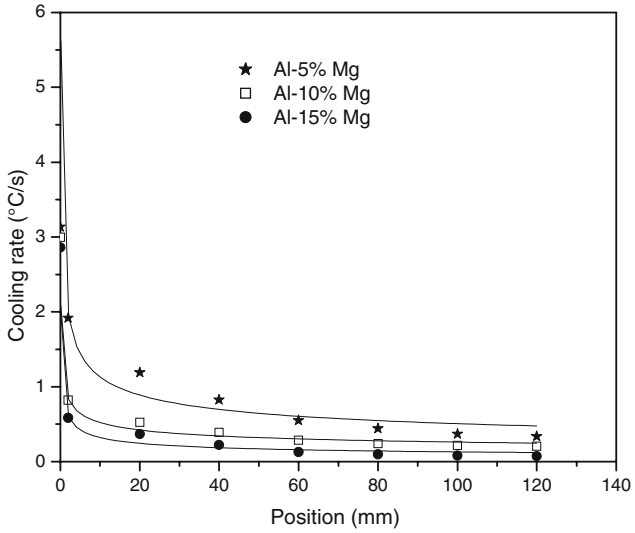

Fig. 8 Variation of the cooling rate (T^*) as function of position of liquidus isotherm for the different Al–Mg alloys

The variations of thermal gradient (G_L) ahead of liquidus isotherm as function of the position of this isotherm for the Al–Mg alloys are shown in Fig. 7. The thermal gradient is obtained from the relation:

$$G_L = \frac{T' - T_L}{x' - x_L} \tag{5}$$

where T_L is liquidus temperature, at liquidus isotherm position (x_L) and T' is the temperature at a position (x') ahead of the liquidus isotherm position. The gradient is higher at the beginning of the solidification process when the superheat of liquid metal is high and decreases rapidly as this superheat is dissipated approaching to zero. It is observed that the gradient is a little higher for higher magnesium contents decreasing slightly as magnesium content decreases. The reason for this behavior is that heat flow in the sample during solidification decreases with magnesium content due to extended mushy zone, as explained previously, attenuating the dissipation of superheat in the liquid metal.

From the results obtained for tip growth rate and thermal gradient, the cooling rate (T^*) associated to the liquidus isotherm front is determined applying the equation [1]:

$$T^* = G_L \cdot v \tag{6}$$

where T^* is the cooling rate, G_L is the thermal gradient, and v is the dendrite tip growth rate. Figure 8 shows the variation of the cooling rate as function of position of liquidus isotherm for the alloys studied. The cooling rate is high at the beginning of the solidification processes but decreases continuously due to the increasing thermal resistance imposed by the crescent air gap at metal/mould interface and the increasing solidified shell. Comparing the results for the three alloys, it is observed that the cooling rate decreases with magnesium content, as consequence of decreasing observed in dendrite tip growth rate (see Fig. 5) for the reasons explained before.

The following results refer to macro and microstructures formation observed during solidification of the Al–Mg alloys.

Figure 9 shows the macrostructures for pure aluminum (a) and for Al 5 wt% Mg (b), Al 10 wt% Mg (c), and Al 15 wt% Mg (d). In this case, results for pure aluminum were added to analyze the effect of magnesium content in columnar zone formation. It is observed that, in spite of some anomalous grains, for pure aluminum the structure is preponderantly columnar in all extension of the solidified specimen, growing in the direction of heat transfer, and for the Al–Mg alloys the extension of the columnar zone decreases as the magnesium content increases. As observed in Fig. 7, thermal gradients increase with magnesium content attenuating the dissipation of superheat and contributing to keep a columnar growth. Figure 10 presents the extension of the columnar zone as function of the magnesium content. It is observed a practically linear variation of the extension of columnar zone with the magnesium content. It is interesting to note that for Al 15 wt% Mg changes in preferential growth direction is observed. These, generally denominated, feathery grains originate close to metal/mould interface where the heat extraction is high. This phenomenon was studied by Henry et al. who attributed it to high thermal gradients and cooling rate [11]. The results obtained in this study indicate that for Al–Mg alloys these changes in growth direction are also affected by the magnesium content, occurring for high values of Mg content.

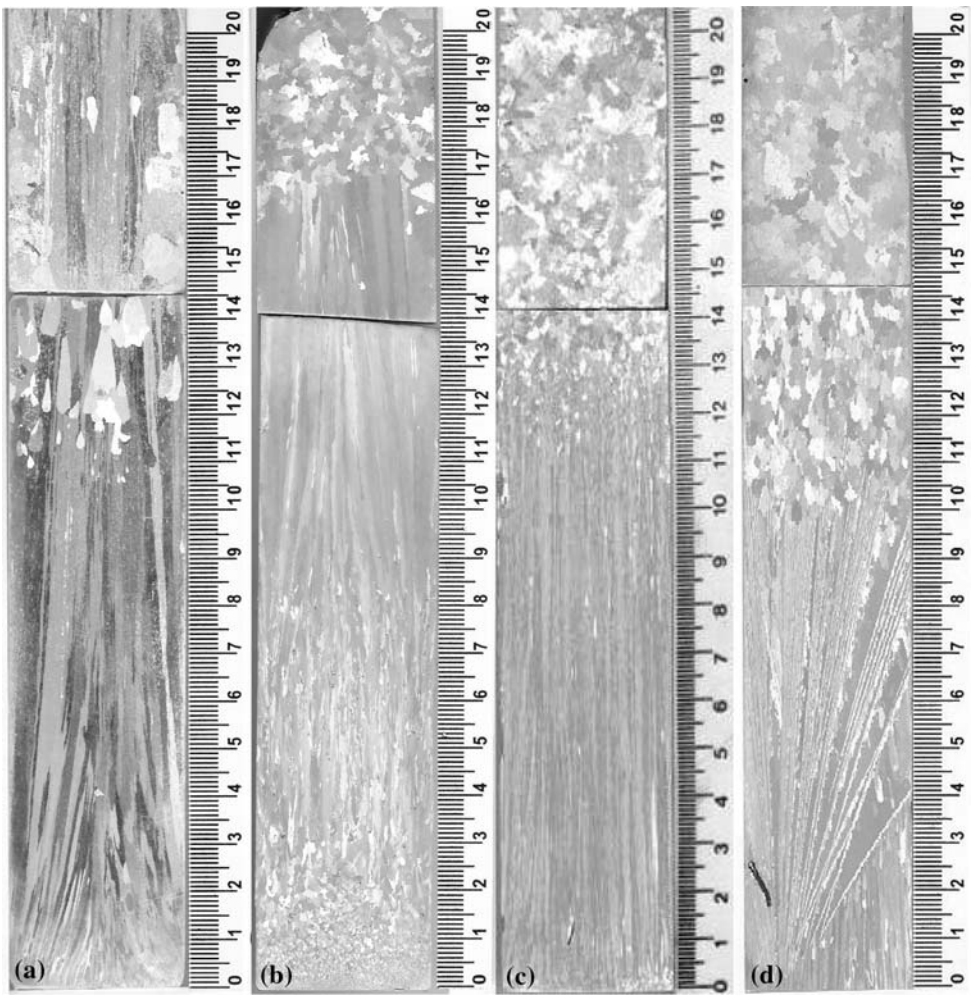

Fig. 9 Macrostructures for pure aluminum (**a**) and for Al 5 wt% Mg (**b**), Al 10 wt% Mg (**c**) and Al 15 wt% Mg (**d**)

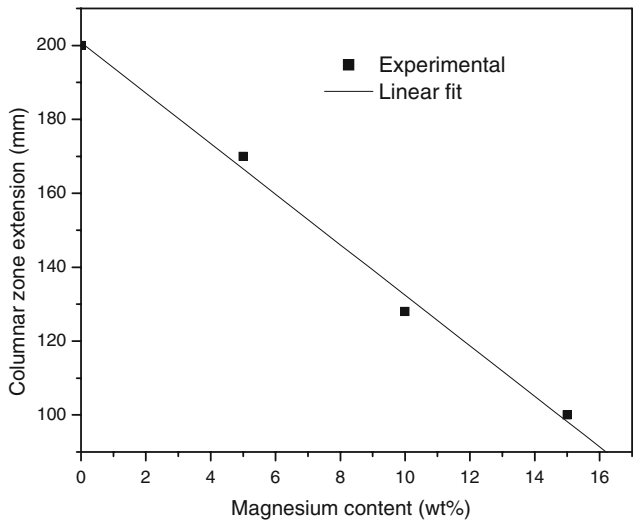

Fig. 10 Extension of the columnar zone as function of the magnesium content

Concerning now to microstructures, Fig. 11 presents the variation of primary dendrite arm spacing (λ_1) as function of position of liquidus isotherm (x), for the alloys containing 5, 10, and 15 wt% Mg. The lines represent the best fit of experimental measurements expressing the dependence between spacing and position as a power function. It is observed that near metal/mould interface, the primary dendrite arm spacing is smaller due to high values of tip growth rate and cooling rate and that spacing increases during the solidification processes as heat transfer coefficient decreases and thermal resistance of solidified shell increases. The dependence of primary arm spacing on alloy content is not yet well established, some authors reported that the primary spacing is little affected by alloy content [7, 16] and others concluded that it increases with alloy content [17]. The results presented at Fig. 11 indicate that for Al–Mg alloys the primary spacing increases with magnesium content, but considering the deviation of the measurements this influence is not very significant.

Considering that for certain alloys, the primary arm spacing predictions furnished by theoretical models concerning to steady-state conditions fit well with the experimental results obtained in unsteady-state conditions [7], the experimental results obtained for the Al–Mg alloys were compared with predictions obtained applying models

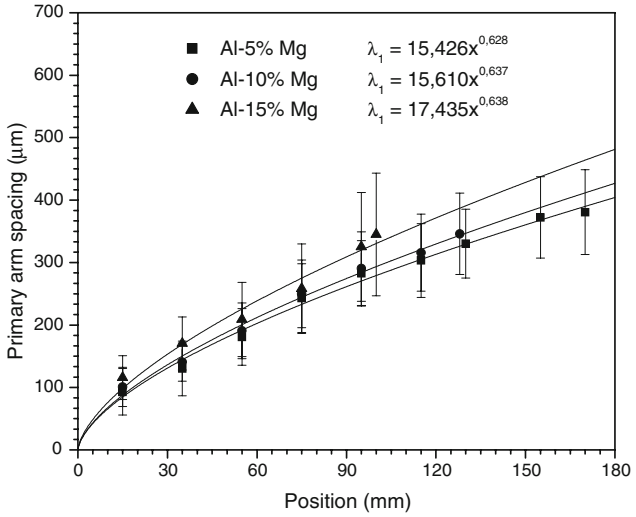

Fig. 11 Variation of primary dendrite arm spacing (λ_1) as function of position of liquidus isotherm (x), for the alloys containing 5, 10 and 15 wt% Mg

proposed by Hunt [18], Kurz and Fisher [1, 19], Trivedi [20] and Geying and Lixin [21]. Basically, the primary arm spacing depends on the product $G^{-0.5}{\cdot}v^{-0.25}$ [1]. Figure 12a–c present the comparisons for the alloys containing 5, 10, and 15 wt% Mg, respectively. The primary arm spacing was plot as function of the product: $G^{-0.5}{\cdot}v^{-0.25}$. It is clear from the results that for the Al–Mg alloys the best fit is obtained using the model proposed by Hunt, which can be applied to predict the primary space for these alloys.

Figure 13 presents the variation of secondary dendrite arm spacing (λ_2) as function of position of liquidus isotherm (x), for the alloys containing 5, 10, and 15 wt% Mg. The lines represent the best fit of experimental measurements expressing the dependence between spacing and position as a power function. In a similar way observed in the behavior of primary arms, near metal/mould interface the secondary dendrite arm spacing is smaller due to high values of tip growth rate and cooling rate and increases during the solidification processes as heat transfer coefficient decreases and thermal resistance of solidified shell increases. The dependence of secondary arm spacing on alloy content is more evident in this case. As the secondary arm spacing depends directly on the local solidification time [1], the results indicate that this spacing increases with magnesium content (see Fig. 6). The experimental results for secondary arm spacing were compared with predictions obtained from theoretical models proposed by Jones [22], Feurer [23] and Kirkwood [24], considering unsteady-state conditions. Figure 14a–c shows the comparisons for the alloys containing 5, 10, and 15% Mg, respectively. The secondary arm spacing was plot as function of the local solidification time. In this case, predictions furnished by

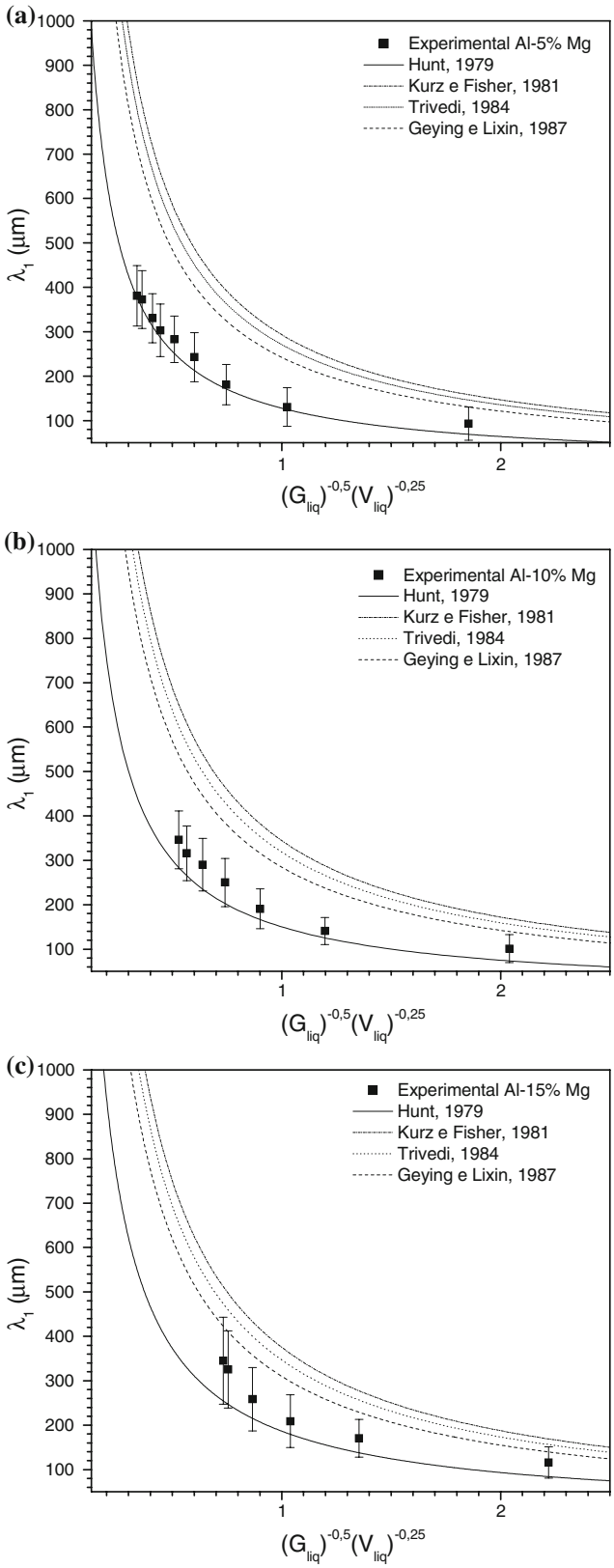

Fig. 12 Comparison between experimental results of primary dendrite arm spacing (λ_1) with predictions obtained applying models existing in the literature for Al 5 wt% Mg (**a**), Al 10 wt% Mg (**b**) and Al 15 wt% Mg (**c**)

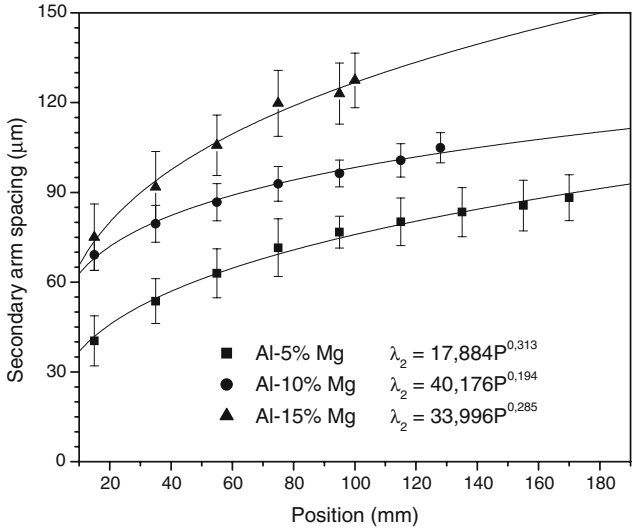

Fig. 13 Variation of secondary dendrite arm spacing (λ_2) as function of position (x), for the alloys containing 5, 10 and 15 wt% Mg

the model proposed by Feurer shows a best fit with experimental results.

Some other correlations can be established between primary and secondary dendrite arm spacing and solidification parameters. Figure 15 shows, adopting logarithm scales, the variation of the primary arm spacing with the cooling rate, for the three Al–Mg alloys studied. As the primary arm spacing varies with the inverse of cooling rate [1], the results indicate that the primary spacing decreases as cooling rate increases. Analogous results are presented in Fig. 16 for secondary dendrite arm spacing. The secondary arm spacing also varies with the inverse of cooling rate [1], decreasing as cooling rate increases.

Conclusions

From the results obtained for unsteady-state unidirectional solidification of Al–Mg alloys containing 5, 10, and 15 wt% Mg, some conclusions were derived and can be summarized as follows.

The global heat transfer coefficient between metal and coolant for the Al–Mg alloys increases significantly as magnesium content increases.

Increasing the magnesium content, which increases the difference between liquidus and solidus temperatures, the time for the dendrite tips reach an equivalent distance also increases.

The dendrite tip growth rate decreases with the distance of metal/mould interface. Increasing the magnesium content, the dendrite tip growth rate decreases.

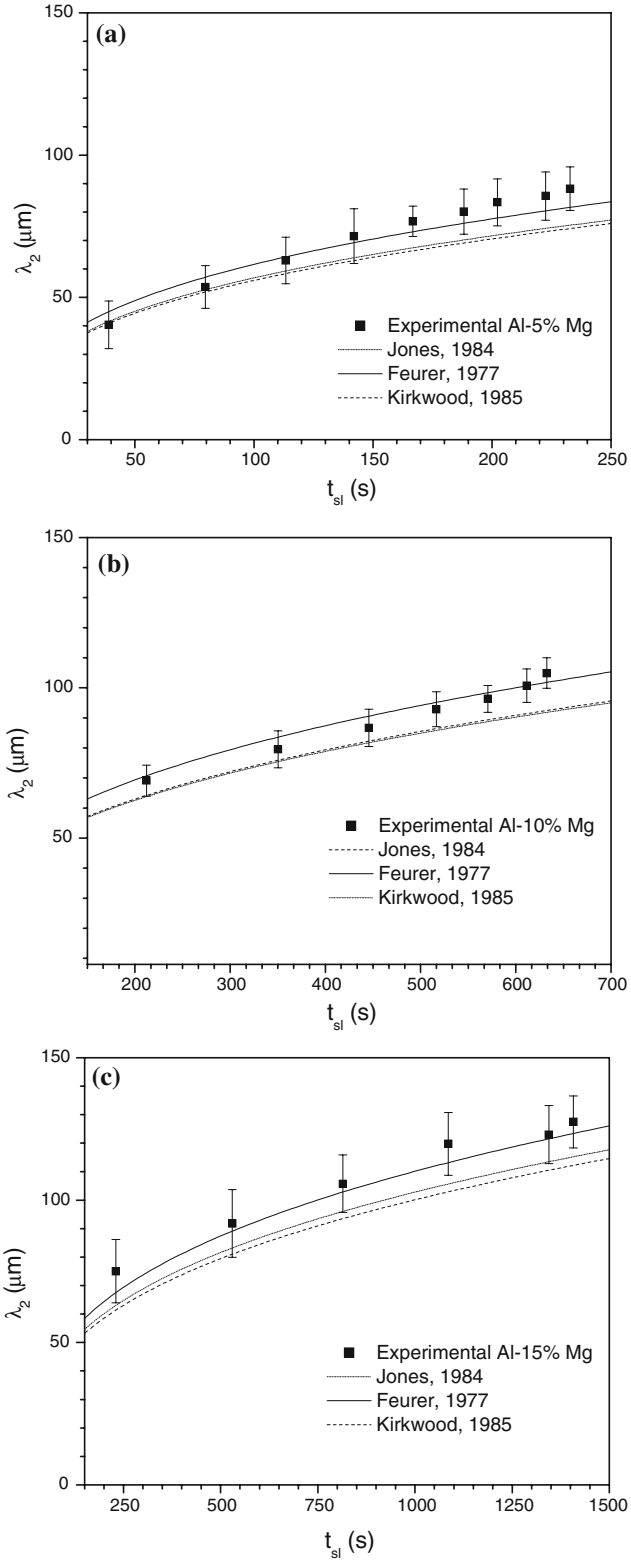

Fig. 14 Comparison between experimental results of secondary dendrite arm spacing (λ_2) with predictions obtained applying models existing in the literature for Al 5 wt% Mg (**a**), Al 10wt% Mg (**b**) and Al 15 wt% Mg (**c**)

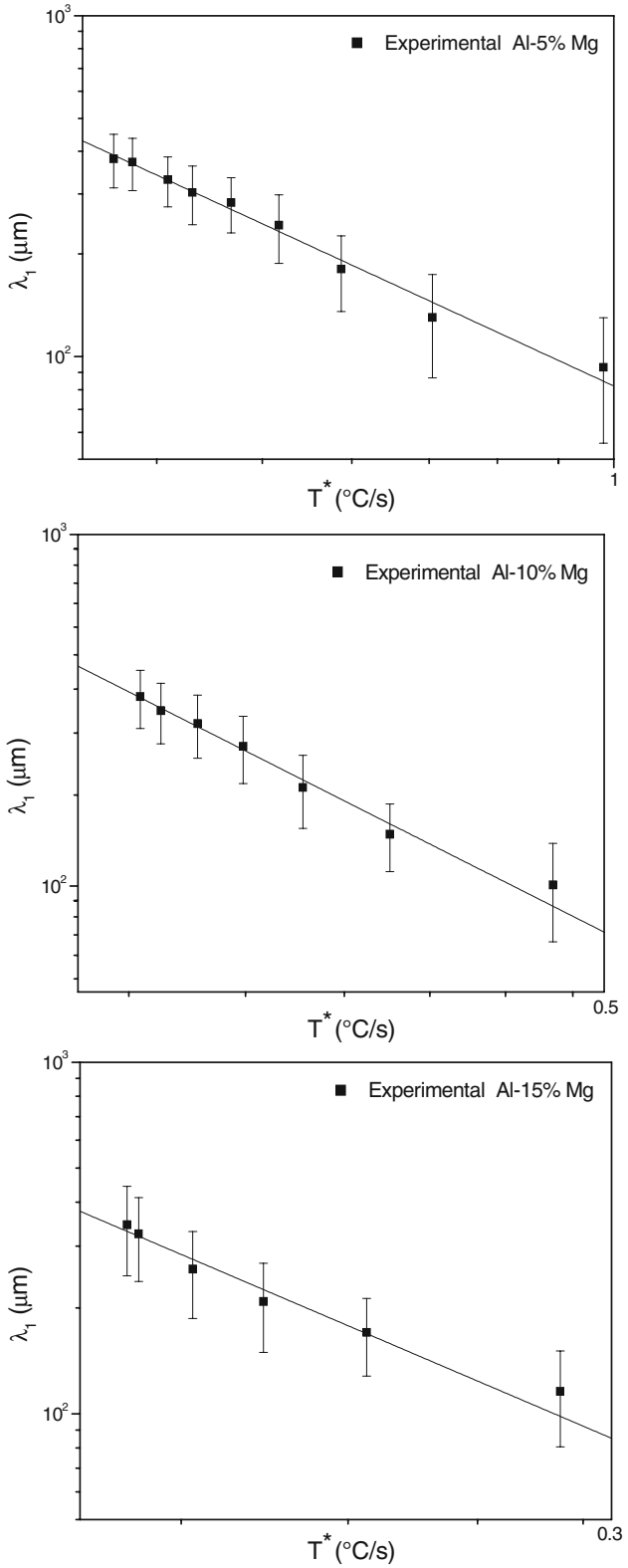

Fig. 15 Variation of the primary arm spacing (λ_1) with the cooling rate (T^*), for the three Al–Mg alloys

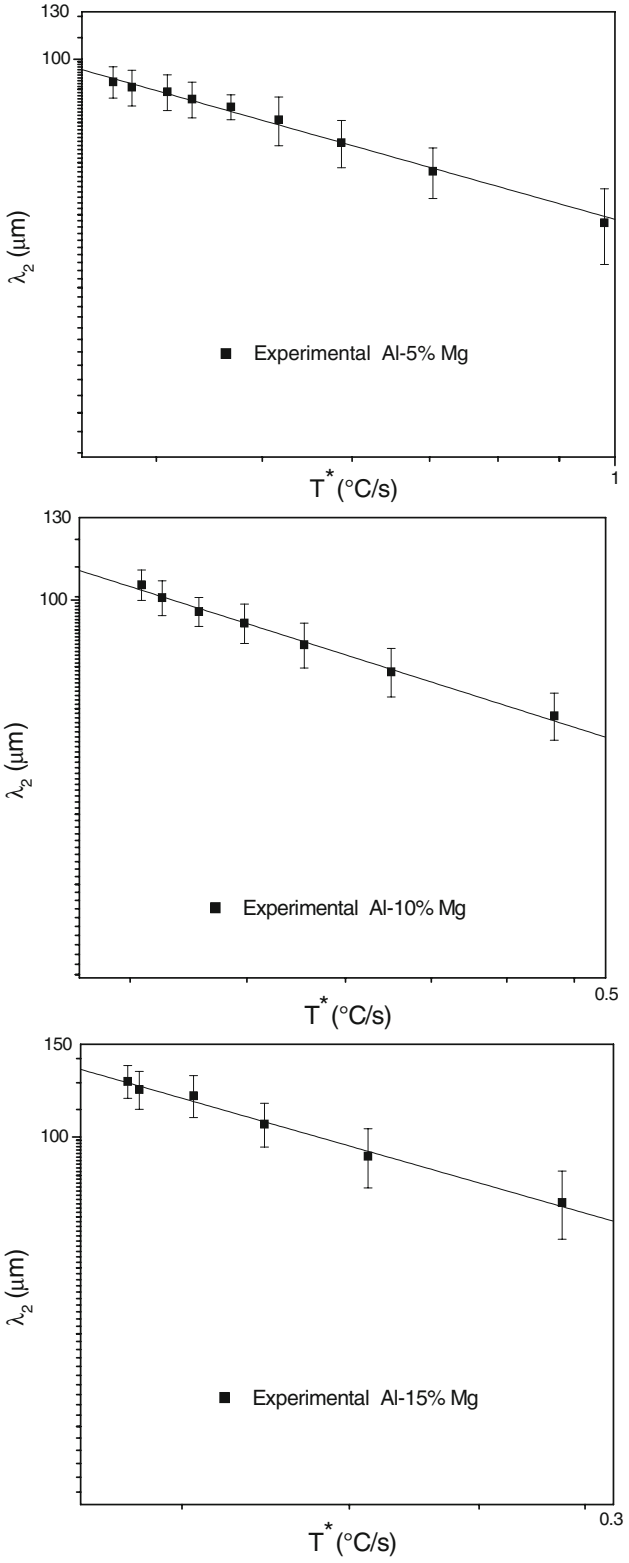

Fig. 16 Variation of the secondary arm spacing (λ_2) with the cooling rate (T^*), for the three Al–Mg alloys

The local solidification time increases with the magnesium content.

The thermal gradient ahead of liquidus isotherm is higher at the beginning of the solidification process, when the superheat of liquid metal is high, and decreases rapidly as this superheat is dissipated approaching to zero. It is observed that the gradient is a little higher for higher magnesium contents decreasing slightly as magnesium content decreases.

The cooling rate associated to the liquidus isotherm front is initially high but decreases continuously during solidification process. The cooling rate decreases with magnesium content.

For pure aluminum, the structure is preponderantly columnar in all extension of the solidified specimen, growing in the direction of heat transfer, and for the Al–Mg alloys the extension of the columnar zone decreases as the magnesium content increases. It is observed that the extension of columnar zone shows a linear variation with the magnesium content.

Concerning to microstructure formation, it is observed that near metal/mould interface, the primary and secondary dendrite arm spacing are smaller, increasing during the solidification processes. Both the primary and secondary dendrite arm spacing increase with magnesium content. For primary dendrite arm spacing the best fit between experimental results and theoretical models is obtained using the model proposed by Hunt and for secondary dendrite arm spacing the best fit is obtained by the model proposed by Feurer. Primary and secondary arms decrease with the cooling rate during solidification.

Acknowledgements The authors acknowledge the financial support provided by CAPES and CNPq (The Brazilian Research Council).

References

1. Kurz W, Fisher DJ (1992) Fundamentals of solidification. Trans Tech, Aedermannsdorf
2. Flemings MC (1974) Solidification processing. McGraw-Hill, New York
3. Bouchard D, Kirkaldy JS (1997) Metall Mater Trans B 28B:651
4. Melo MLNM, Rizzo EMS, Santos RG (2005) J Mater Sci 40:1599. doi:10.1007/s10853-005-0659-y
5. Melo MLNM, Rizzo EMS, Santos RG (2004) Mater Sci Eng A 374:351
6. Rocha OL, Siqueira CA, Garcia A (2003) Mater Sci Eng A 347:59
7. Rocha OL, Siqueira CA, Garcia A (2003) Metall Mater Trans A 34A:995
8. Gündüz M, Çadirli E (2002) Mater Sci Eng A 327:167
9. Whitesell HS, Overfelt RA (2001) Mater Sci Eng A 318:264
10. Lin X, Huang W, Feng J, Li T, Zhou Y (1999) Acta Mater 47:3271
11. Henry S, Minghetti T, Rappaz M (1998) Acta Mater 46:6431
12. Taler J (1992) Trans ASME 114:1048
13. Rappaz M, Stefanescu DM (1988) Metals handbook, vol 15. ASM, Ohio
14. Scheil E (1942) Zeitschrift fur Metalkunde 34:70
15. Pehlke RD, Jeyarajan A, Wada H (1982) Summary of thermal properties of casting alloys and mold materials. University of Michigan, Ann Arbor
16. Sharp RM, Hellawell A (1969) J Cryst Growth 5:155
17. Okamoto T, Kishitake K (1975) J Cryst Growth 29:137
18. Hunt JD (1979) Solidification and casting of metals. The Metals Society, London
19. Kurz W, Fisher JD (1981) Acta Metall 29:11
20. Trivedi R (1984) Metall Mater Trans A 15A:977
21. Geying A, Lixin L (1987) J Cryst Growth 80:383
22. Jones H (1984) Proceedings of solidification processing, Sheffield, p 349
23. Feurer U (1977) Proceedings of the symposium on quality control of engineering alloys, Delft, p 131
24. Kirkwood DH (1985) Mater Sci Eng 73:51